Electronic Supplementary Information

for

Systematic Truncating Aptamers to Create High Performance Graphene Oxide (GO)-based Aptasensors for Multiplex Detection of Mycotoxins

Xinglin Wang,[†] Xiaoyi Gao,[†] Jiale He,[†] Xiaochen Hu,[†] Yunchao Li,[*,†] Xiaohong Li,[†] Louzhen Fan,[†] and Hua-Zhong Yu[*, ‡]

[†]*College of Chemistry, Beijing Normal University, Beijing 100875, P. R. China*

[‡]*Department of Chemistry, Simon Fraser University, Burnaby, British Columbia V5A 1S6, Canada*

* Corresponding authors: liyc@bnu.edu.cn (Y.L.), hogan_yu@sfu.ca (H.Y.)

Additional experimental data include truncated aptamer sequences, experimental condition optimization, fluorescence titration curves, detection selectivity tests, real-world sample detection, and the results of the dual-channel DNA/GO aptasensor.

Table S1 Sequences of the oligonucleotides (from 5'- to 3'-end) used in the present study. The constant base sequences are underlined, i.e., these bases have been kept for the truncation experiments.

DNA strand	Sequence (from 5'- to 3'-end)
P-AFB1-50	**GTT GGG CAC GTG TTG TCT CTC TGT GTC TCG TGC CCT TCG CTA GGC CCA CA**
P-AFB1-46	**GTT GGG CAC GTG TTG TCT CTC TGT GTC TCG TGC CCT TCG CTA GGC C**
P-AFB1-40	**GTT GGG CAC GTG TTG TCT CTC TGT GTC TCG TGC CCT TCG C**
P-AFB1-35	**GTT GGG CAC GTG TTG TCT CTC TGT GTC TCG TGC CC**
P-AFB1-31	**GTT GGG CAC GTG TTG TCT CTC TGT GTC TCG T**
P-AFB1-37	**GGG CAC GTG TTG TCT CTC TGT GTC TCG TGC CCT TCG C**
P-AFB1-34	**CAC GTG TTG TCT CTC TGT GTC TCG TGC CCT TCG C**
P-AFB1-30	**TG TTG TCT CTC TGT GTC TCG TGC CCT TCG C**
P-OTA-61	**TGGTGGCTGTAGGTCAGCATCTGATCGGGTGTGGGT GGCGTAAAGGGAGCATCGGACAACG**
P-OTA-48	**TCAGCATCTGATCGGGTGTGGGTGGCGTAAAGGGAG CATCGGACAACG**
P-OTA-36	**GAT CGG GTG TGG GTG GCG TAA AGG GAG CAT CGG ACA**

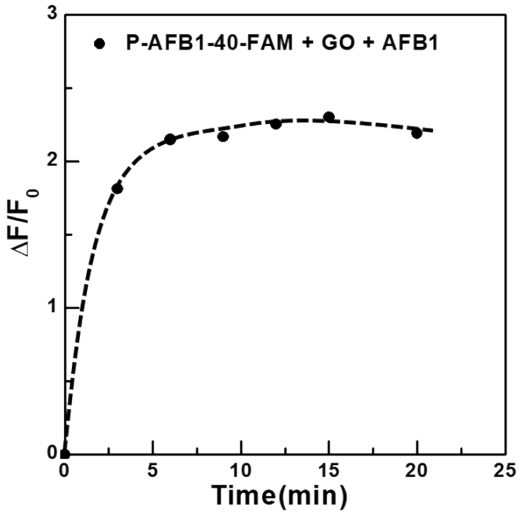

Fig.S1 Optimization of the incubation time of P-AFB1-40-FAM/GO solution (100 nM P-AFB1-40-FAM, 16 μg mL^{-1} GO) upon addition of 100 ng mL^{-1} AFB1.

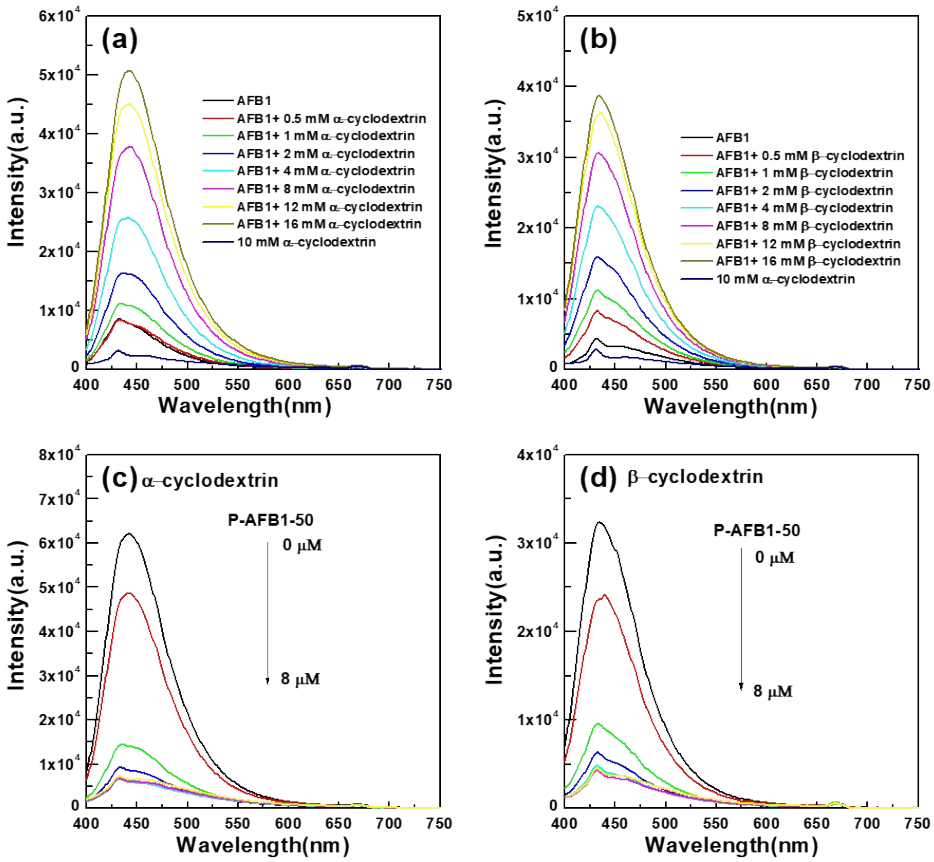

Fig. S2 The optimization of the type (α-cyclodextrin and β-cyclodextrin) and the concentration of cyclodextrin. The enhanced fluorescence of AFB1 in the presence of various concentrations of (a) α-cyclodextrin and (b) β-cyclodextrin. The competitive reaction of P-AFB1-50 with (c) 160 nM AFB1 incubating with 12 mM α-cyclodextrin, and (d) 160 nM AFB1 incubating with 12 mM β-cyclodextrin.

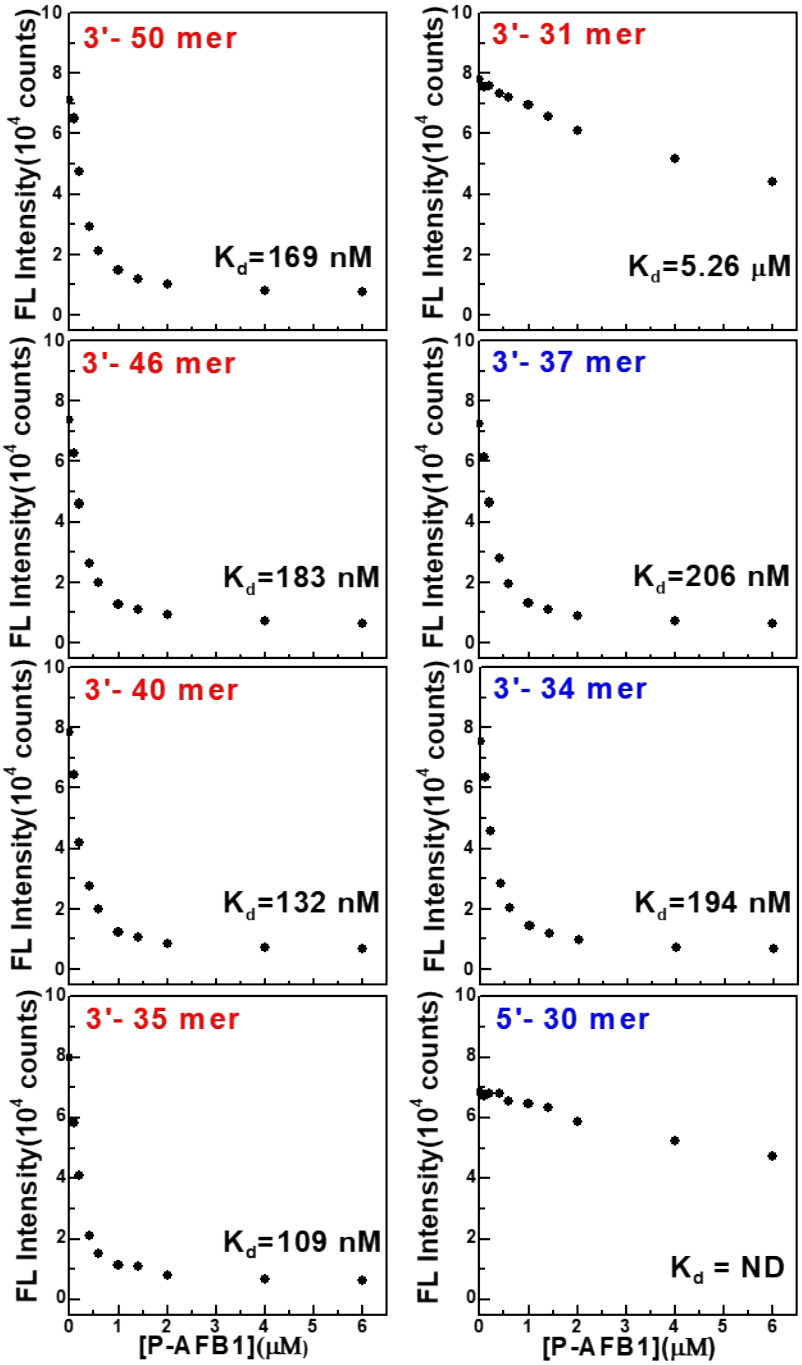

Fig. S3 Fluorescence titration curves of the truncated aptamers of different lengths. These curves were recorded by using the truncated aptamers of various concentration to titrate the stock solutions containing 160 nM AFB1 and 12 mM α-cyclodextrin. The sequences of the truncated versions of the aptamer are shown in Fig. 1 and Table S1.

Table S2 Determination of AFB1 in spiked 1% white wine samples. This experiment is representative of three replicate experiments. "RSD" means the relative standard derivation of three parallel measurements.

Sample	Spiked (ng/mL)	Measured by our method (ng/mL)	Recovery (%)	RSD (%)	Measured by HPLC (ng/mL)
1	15.0	14.6	97.3	6.7	15.18
2	40.0	41.8	104.5	7.6	39.20
3	60.0	56.7	94.5	8.7	59.89

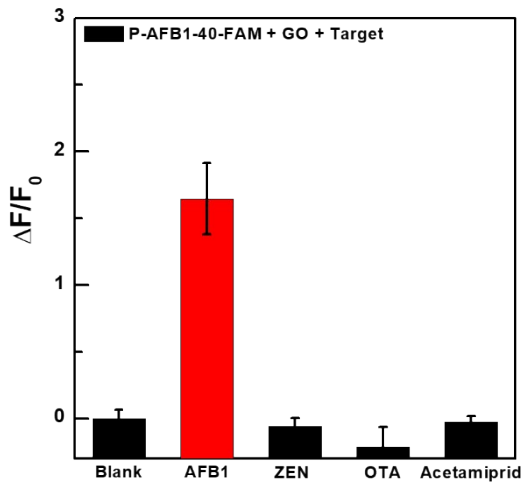

Fig. S4 Selectivity of the DNA/GO sensing platform based on the truncated aptamer P-AFB1-40 for AFB1 (100 ng mL^{-1}) over other food contaminants (ZEN, OTA, Acetamiprid, each at a concentration of 1.0 μg mL^{-1}).

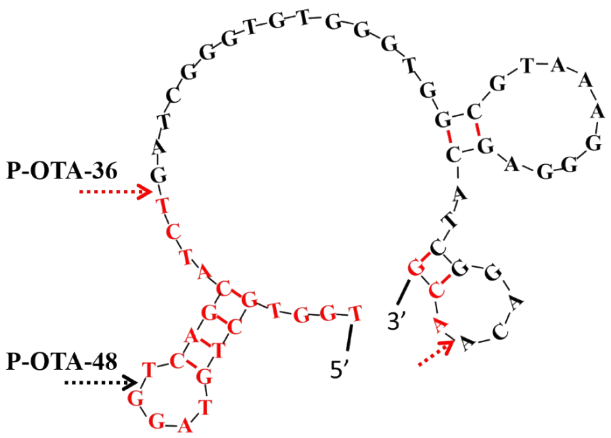

Fig. S5 The secondary structure predicted by mfold program for P-OTA-61 (the original sequence reported in ref. 34). Extraneous nucleotides were removed sequentially from 5'- end (or 3' - end) to create two representative truncated versions of the aptamer (P-OTA-48 and P-OTA-36).

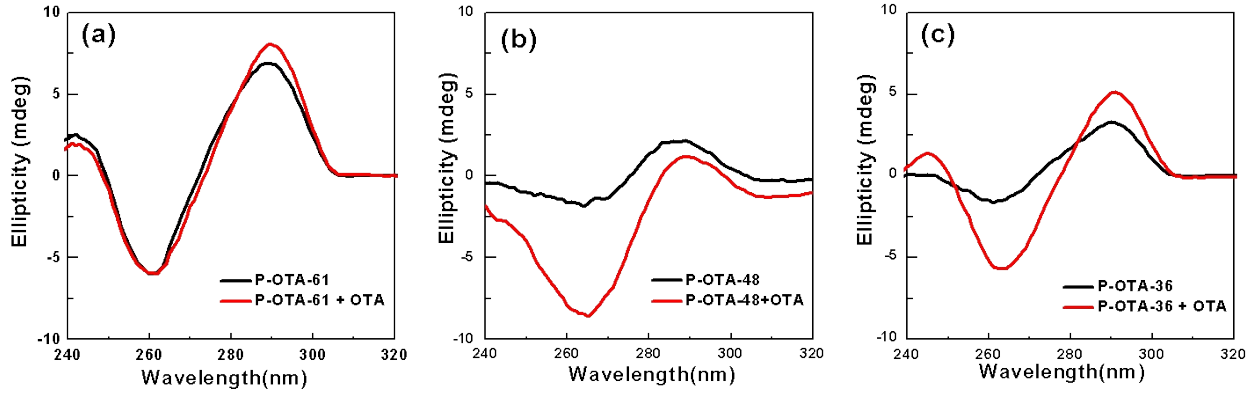

Fig. S6 CD spectra of the truncated aptamers (1.0 μM) of different sequence lengths in the absence (black line) and presence (red line) of OTA (1.0 μM). (a) P-OTA-61; (b) P-OTA-48; (c) P-OTA-36.

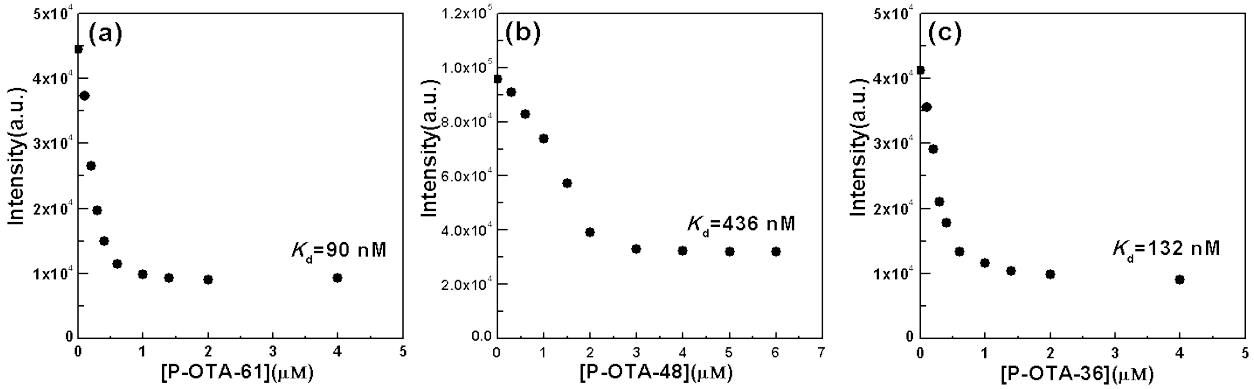

Fig. S7 Fluorescence titration curves of the truncated aptamers of different sequence lengths. (a) P-OTA-61; (b) P-OTA-48; (c) P-OTA-36. These curves were recorded by using the truncated aptamers of various concentration to titrate the stock solutions containing 200 nM OTA.

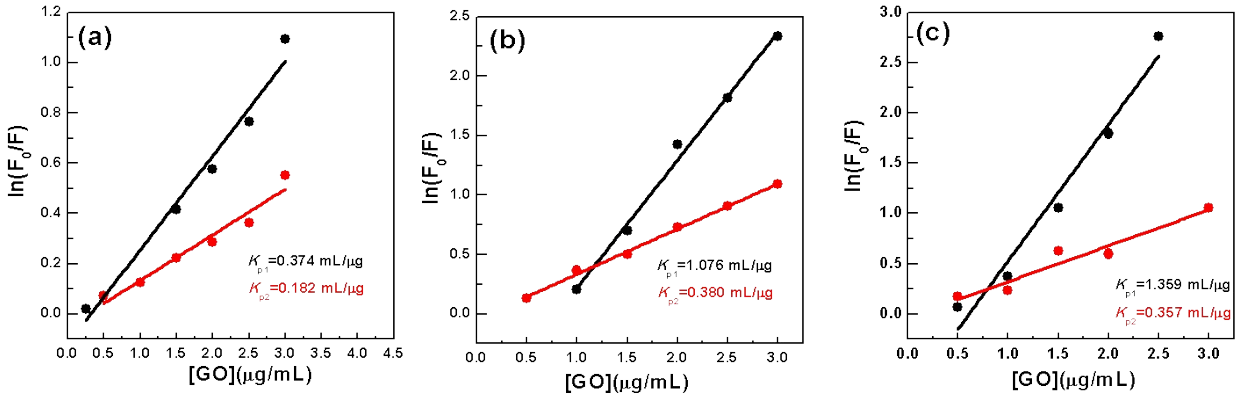

Fig. S8 Plots of $\ln(F_0/F)$ vs. [GO] for the bindings of truncated aptamers with GO in the absence (black line) and presence (red line) of OTA. (a) P-OTA-61; (b) P-OTA-48; (c) P-OTA-36.

Table S3 Parameters characterizing the quenching of truncated aptamers (K_{p1}) and aptamer/OTA conjugates (K_{p2}) by GO (K_p is quenching constant).

Aptamer	K_{P1} (mL μg^{-1})	K_{P2} (mL μg^{-1})	K_{P1}/K_{P2}
P-OTA-61	0.374	0.182	2.06
P-OTA-48	1.076	0.380	2.83
P-OTA-36	1.356	0.357	3.80

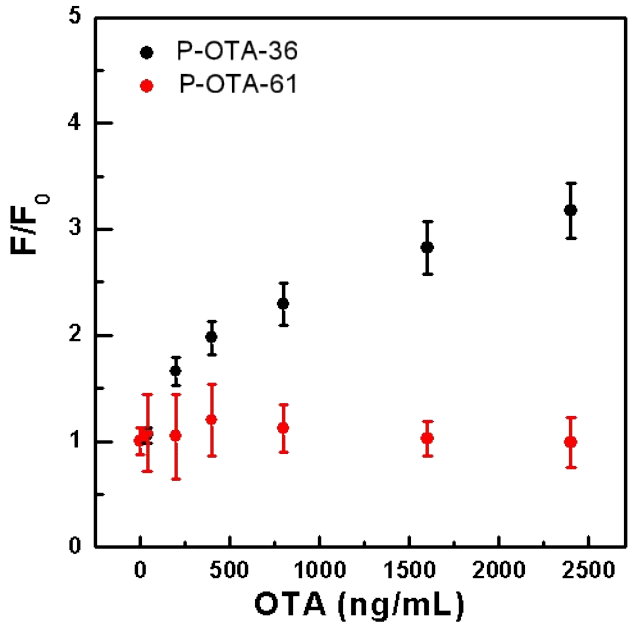

Fig. S9 Comparison of the analytical performance of the GO-based aptasensors using P-OTA-61 or P-OTA-36 as the probe for the detection of OTA. The experimental uncertainties (error bars) were obtained from three independent replicate samples.

.

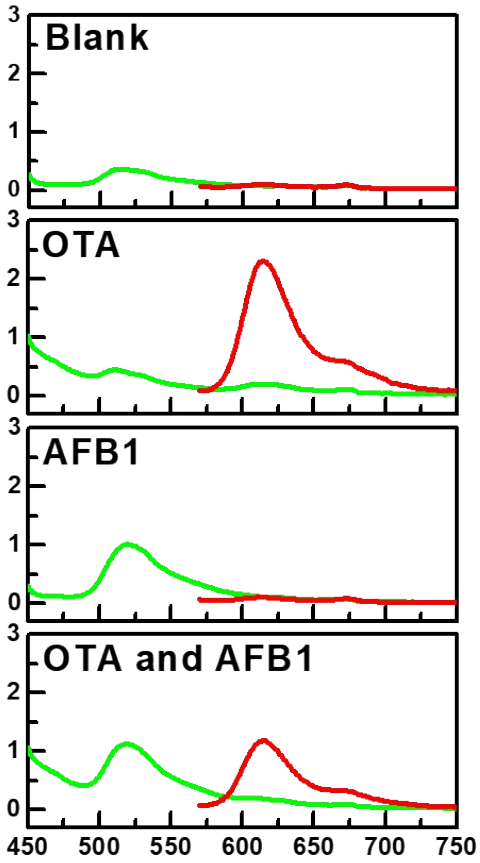

Fig.S10 Validation of the feasibility of the application of dual-channel DNA/GO fluorescence platform for the simultaneous detection of OTA and AFB1. This dual-channel sensing platform was constructed by mixing 60 nM P-AFB1-40-FAM, 180 nM P-OTA-36-Texas red and 16 μg mL^{-1} GO together. The concentrations of AFB1 and OTA testing were 1.0 μg mL^{-1} and 4.0 μg mL^{-1}, respectively.